C. elegans pro-1 activity is required for soma/germline interactions that influence proliferation and differentiation in the germ line

Darrell J. Killian and E. Jane Albert Hubbard*

Department of Biology New York University, New York, NY 10003, USA
*Author for correspondence (e-mail: jane.hubbard@nyu.edu)

Accepted 25 November 2003

Development 131, 1267-1278
Published by The Company of Biologists 2004
doi:10.1242/dev.01002

Summary

Strict spatial and temporal regulation of proliferation and differentiation is essential for proper germline development and often involves soma/germline interactions. In *C. elegans*, a particularly striking outcome of defective regulation of the proliferation/differentiation pattern is the Pro phenotype in which an ectopic mass of proliferating germ cells occupies the proximal adult germ line, a region normally occupied by gametes. We describe a reduction-of-function mutation in the gene *pro-1* that causes a highly penetrant Pro phenotype. The *pro-1* mutant Pro phenotype stems from defects in the time and position of the first meiotic entry during early germline development. *pro-1(RNAi)* produces a loss of somatic gonad structures and concomitant reduction in germline proliferation and gametogenesis. *pro-1* encodes a member of a highly conserved subfamily of WD-repeat proteins. *pro-1(+)* is required in the sheath/spermatheca lineage of the somatic gonad in its role in the proper establishment of the proliferation/differentiation pattern in the germline. Our results provide a handle for further analysis of this soma-to-germline interaction.

Key words: Germline, Meiosis, Proliferation, Somatic gonad, *C. elegans*

Introduction

In many species, communication between the somatic gonad and germ cells is required to produce a functional reproductive system. In particular, interactions with the somatic gonad influence the control of germline proliferation and differentiation, and the molecular mechanisms underlying these interactions are under intense research (for a review, see Spradling et al., 2001). In male mammals, for example, a signal from the developing male somatic gonad prevents premature meiotic entry. Later, germline stem cells are maintained by contact with a somatic niche, and differentiation progresses once germ cells move out of the niche (for reviews, see Kiger and Fuller, 2001; Brinster, 2002; McLaren, 2003).

Germline development in *Caenorhabditis elegans* hermaphrodites shares phenomenological parallels with that of male mammals. Interactions with the developing somatic gonad influence the time and position of early germline proliferation and differentiation, and a spatially restricted population of stem cells maintains the adult germ line (Kimble and Hirsh, 1979; Kimble and White, 1981). *C. elegans* gonadogenesis is relatively simple and is amenable to genetic analysis, offering an attractive system to investigate soma/germline interactions (Fig. 1). During early germline development, all germ cells are proliferative. In the third larval stage (L3), the proximal-most germ cells enter meiosis (‘initial meiosis’; Fig. 1). Initial meiosis establishes a border: subsequent proliferation occurs distal to the border and differentiation (meiotic development) proceeds proximally from it. Transition (early prophase of meiosis I) and pachytene nuclei appear in the L3, and gametogenesis occurs in the late L4 and adult. In the adult, sperm and oocytes accumulate in the proximal germ line. The formation and maintenance of this distal-to-proximal, proliferation/differentiation pattern requires somatic gonad/germline interactions (Kimble and White, 1981).

The best-characterized somatic gonad/germline interaction in *C. elegans* is the distal tip cell (DTC)/germline interaction. This interaction promotes mitosis and/or inhibits meiosis in the distal germ line (Kimble and White, 1981). Ablation of the DTC by laser microsurgery causes all germ cells to enter meiosis. The GLP-1 receptor in the germ line, a member of the LIN-12/Notch family, mediates the interaction by binding LAG-2, a DSL family ligand expressed in the DTC (Austin and Kimble, 1987; Lambie and Kimble, 1991; Tax et al., 1994; Henderson et al., 1994). Early in development, two cells of the proximal somatic gonad, the anchor cell (AC) precursors, also produce LAG-2 and contribute to continued early germline proliferation (Pepper et al., 2003b).

Other non-DTC, non-AC soma/germline interactions influence robustness of germline proliferation and meiotic progression (McCarter et al., 1997). Ablation of both spermatheca/sheath precursor cells (SS cells; Fig.1) on one side of the gonad at the L2/L3 molt reduces germline proliferation, meiotic progression, and gametogenesis (McCarter et al., 1997). This ablation significantly reduces germline proliferation even when GLP-1 is constitutively active, suggesting that it acts parallel to DTC/germline signaling mediated by GLP-1 (McCarter et al., 1997).

Ablation of the SS/dorsal uterus precursors (SS/DU, Z1.pa and Z4.ap; Fig. 1) in the late L1 together with ventral uterine

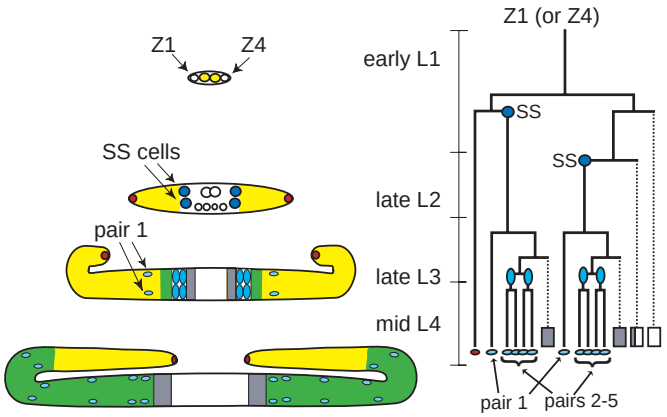

Fig. 1. Selected stages and lineages of hermaphrodite germline and somatic gonad development. Schematic diagram depicting four stages of gonadogenesis (left) and a corresponding abbreviated lineage (right). Yellow indicates germline proliferation; green indicates meiotic development. Somatic gonad lineages are coded: red, DTC; dark blue, SS cells; cyan, differentiated sheath cells; gray, spermatheca; white, uterus (Kimble and Hirsh, 1979); broken lines indicate additional cell divisions. The germ line is largely syncytial; 'germ cell' refers to each nucleus and surrounding cytoplasm.

precursor cells (VUs) causes a more dramatic defect: proximal proliferation (Pro) (Seydoux et al., 1990). The Pro phenotype is characterized by a mass of proliferating germ cells (or 'tumor') in the proximal part of the adult gonad. Thus the normal distal-to-proximal developmental pattern is altered without affecting germline cell fates per se. Mutants that display a Pro phenotype include loss-of-function mutations in *lin-12* (Seydoux et al., 1990), *ego-3* (Qiao et al., 1995), *gld-2* (Kadyk and Kimble, 1998) and *puf-8* (Subramaniam and Seydoux, 2003), and gain-of-function *glp-1(Pro)* mutants (Pepper et al., 2003a). *lin-12* acts in the somatic gonad (Seydoux et al., 1990), whereas *gld-2*, *puf-8* and *glp-1* act in the germ line (Austin and Kimble, 1987; Kadyk and Kimble, 1998; Subramaniam and Seydoux, 2003).

Two distinct developmental errors can lead to a Pro phenotype: (1) a reversion from meiotic development to mitosis and (2) a defect in initial meiosis. An example of the first defect is the *puf-8* Pro phenotype. When *puf-8* activity is reduced, germ cells proliferate, enter meiosis at the correct time and position, and differentiation proceeds through meiotic prophase. As germ cells begin spermatogenesis, however, some fail to complete a reductional division and instead return to mitosis. Thus, the tumor in *puf-8* Pro animals derives from cells that entered meiosis but reverted to mitosis (Subramaniam and Seydoux, 2003). By contrast, in *glp-1(Pro)* mutants, proximal-most mitotic cells derive from a population of early germ cells that fail to enter meiosis and, instead, continue to proliferate. Meiosis eventually occurs distal to the tumor, in the normal pattern from the distal tip, resulting in a tumor proximal to gametes (Pepper et al., 2003b).

The *glp-1(Pro)* phenotype is partially dependent on proximal LAG-2-producing cells, suggesting that these mutations render the GLP-1 receptor particularly sensitive to proximal sources of LAG-2 (Pepper et al., 2003b). The establishment of *lin-12(loss-of-function)* Pro phenotype is also AC-dependent, as is the Pro phenotype resulting from select SS/DU/VU ablations mentioned above (Seydoux et al., 1990). Consistent with the possibility that the ablation-induced Pro phenotype is due to inappropriate signaling to the germ line, the phenotype is dependent on *glp-1* activity and on the presence of at least one cell capable of forming an AC (Seydoux et al., 1990).

We introduce *pro-1*, a gene identified by an hypomorphic (reduction-of-function) mutation, *pro-1(na48)*, that causes a highly penetrant Pro phenotype. Our analysis indicates that the *pro-1(na48)* Pro phenotype emanates from faulty temporal and spatial patterning of initial meiosis. Unlike previously described Pro mutants with this etiology, the *pro-1(na48)* Pro phenotype is AC independent. We demonstrate that *pro-1(+)*activity is required in the sheath/spermatheca lineage of the somatic gonad to prevent proximal proliferation in *pro-1(na48)* mutants. A stronger depletion of *pro-1* activity (by RNAi) severely disrupts somatic gonad development. *pro-1* encodes the only *C. elegans* member of a subfamily of WD-repeat-containing proteins that are essential in both budding yeast and fission yeast, but have not been previously characterized in multicellular organisms. Our results point to a previously uncharacterized *pro-1(+)*-dependent role for the sheath/spermatheca lineage in the spatial patterning of early germline proliferation and differentiation.

Materials and methods

Strains and genetic manipulations

Strains were derived from the Bristol strain N2, grown at 25°C unless otherwise noted, and constructed using standard procedures (Brenner, 1974). Mutations used [from Brenner (unless noted) (Brenner, 1974)] are as follows.

LGI: *mpk-1(ga111)* (Lackner and Kim, 1998), *unc-79(e1068)* (Morgan et al., 1990), *rrf-1(pk1417)* (Sijen et al., 2001).

LGII: *unc-4(e120), bli-1(e769), mIn1[dpy-10(e128) mIs14]* (Edgley and Riddle, 2001), *mIs14* is *ccEx9747* (*myo-2* and *pes-10* promoters and a gut enhancer fused individually to GFP) integrated into *mIn1[dpy-10], mnDf58* (Sigurdson et al., 1984).

LGIII: *dpy-17(e164), glp-1(e2141)* (Kodoyianni et al., 1992), *glp-1(ar202)* (Pepper et al., 2003a), *lin-12(n302)* (Greenwald et al., 1983).

LGIV: *fem-1(hc17)* (Nelson et al., 1978).

LGV: *him-5(e1490)*.

Isolation, mapping and molecular identification of *pro-1(na48)*

pro-1(na48) was isolated in an ethyl methane sulfonate mutagenesis (Pepper et al., 2003a). Three-factor and single nucleotide polymorphism mapping (see Wormbase, http:// www.wormbase.org for details) placed *pro-1(na48)* within a 120 kb interval on linkage group II. PCR-amplified R166.4 from *pro-1(na48)* genomic DNA was directly sequenced (DNA Analysis and Sequencing Facility, Columbia University, NY), and a single base pair change G to A [(GAC) to (AAC)] was verified on both strands. Three full-length cDNAs were sequenced (gifts of Y. Kohara; yk1113c3, yk898h5, yk755f10). All splice junctions were identical to the predicted cDNA sequence in Wormbase.

Phenotypic analysis of *pro-1(na48)* and *pro-1(RNAi)*

With the exception of *pro-1(RNAi)*, all data in Tables 1 and 2 were collected after synchronization by hatch-off as described (Pepper et al., 2003a). For Table 1, *pro-1(+)* and *pro-1(+)/pro-1(na48)* live animals were scored at the adult molt for Pro, Mig, vulval phenotypes and for the presence of gametes. Animals of all other genotypes were similarly scored 18 hours (25°C), 22 hours (20°C) and 24 hours

(15°C) after the adult molt. *pro-1(RNAi)* animals were scored as asynchronous adults. RNAi feeding was performed as described previously (Timmons et al., 2001). L4 hermaphrodites were placed onto RNAi plates, transferred, and progeny from the second day were scored as adults. For Table 2, animals were scored after fixation and DAPI staining at stages/times indicated.

Cell ablations

Self-progeny of *pro-1(na48)/mIn1* animals were raised at 25°C and synchronized. After 25 hours, *pro-1(na48)* homozygotes were immobilized on agar pads containing sodium azide, and staged for the presence of Z1.pp and Z4.aa. These cells were then ablated (operated animals) or not (unoperated controls). Adults were scored 48 hours post-ablation for vulval morphology and Pro. Operated animals with any vulval induction were excluded from the analysis. The overall reduced penetrance of the Pro phenotype in both ablated and control animals is likely to be due to slightly lower temperature and azide treatment during the ablation.

Plasmid constructions for mutant rescue and RNAi

pGC16 (*pro-1* rescuing construct)

A PCR product containing R166.4 genomic sequence plus 3318 bp upstream of the start and 560 bp after the stop was inserted into pCR-XL-TOPO (Invitrogen). The insert contains two changes (G to A and G to T at positions –3230 and –342). *unc-4 pro-1/mIn1* hermaphrodites were injected with pGC16 and pRF4[*rol-6(su1006)*] (Mello and Fire, 1995) or pGC16, pRF4 and pTG96[*sur-5::GFP*] (Yochem et al., 1998) at 20 ng/µl, 100 ng/µl and 120 ng/µl respectively. Lines (*naEx1* and *naEx2*, respectively) were generated from fertile F2 Rol Unc animals. Unc non-Rol offspring were Pro. Neither pRF4 nor pTG96 rescues alone (7 and 3 lines, respectively).

pGC15 (*pro-1(RNAi)* feeding construct)

*Acc*I/*Pst*I fragment (2.0 kb) of amplified R166.4 genomic DNA was ligated into *Acc*I/*Pst*I sites in L4440 (Timmons and Fire, 1998). The first intron of the R166.4 contains significant homology to other *C. elegans* genomic sequences and was excluded.

Reporter constructs, expression constructs and immunohistochemistry

ajm-1::GFP (SU93) (Koppen et al., 2001) marks adherens junctions and *lim-7::GFP* (DG1575) marks gonadal sheath cell pairs 1-4 (Hall et al., 1999). Anti-CEH-18 (Greenstein et al., 1994) recognizes DTC and sheath nuclei. Anti-PGL-1 (Kawasaki et al., 1998) (1:5000) marks germ cells. Non-oocyte cells labeled by anti-phospho-histone H3 (Upstate Biotechnology; 1:3000) but not anti-MSP (Miller et al., 2001) (1:1000) are in M phase of mitosis. Gonad dissections, fixation and immunohistochemistry were carried out as described (Pepper et al., 2003b).

pGC29 (*pro-1* promoter driving GFP): (1) 3318 bp upstream of *pro-1* (including the ATG) was amplified from pGC16 (*att*B1, *att*B2 sites in the primers) and recombined into *att*P1, *att*P2 sites in pDONR221 (Invitrogen) to make pGC22. pGC22 was recombined with pPD117.01GtwyGFP (gift of B. Grant) that contains a Gateway donor cassette (*att*R1, *att*R2 in reading frame B ligated into a blunted *Asp*718 site) upstream of GFP and the *let-858* 3′UTR. pGC29 and pRF4 were injected at 100 µg/ml each to generate lines. The following were examined for GFP expression: the somatic gonad (DTC, sheath, spermatheca, and uterus), coelomocytes, hypodermis (tail tip, seam cells), vulva, intestine, unidentified neurons, excretory cell, body wall and pharyngeal muscles.

Mosaic analysis

Mosaic analysis was performed with *unc-4 pro-1(na48); naEx2[pro-1(+), sur-5::GFP, rol-6(su1006)]*. Animals with the array were Unc Rol GFP positive. Animals without the array were Pro non-Rol GFP negative (or non-Pro *pro-1(na48)* phenotypes; Table 1). Adult mosaic non-Pro animals were identified as fertile GFP mosaics. Adult mosaic Pro animals were identified as rare Pro, GFP-positive worms. Cells were scored for GFP fluorescence as follows: AB, the ventral nerve cord and anterior hypodermis nuclei; E, the intestine; MS, the somatic gonad and coelomocytes; C, C-specific body wall muscles and hyp 11; D, D-specific body wall muscles; P4, progeny. For mosaics within the MS lineage, each arm was scored independently (DTC, sheath, spermatheca). The uterine lineage could not be reliably scored in adults, hence losses within Z1.p and Z4.a lineages were not further resolved. Losses within Z1.a or Z4.p-derived spermatheca/sheath lineages versus Z1.p or Z4.a-derived spermatheca/sheath lineages could be distinguished by GFP in the DTC (Z1.aa or Z4.pp).

Results

The *pro-1(na48)* mutation interferes with germline pattern

We obtained *pro-1(na48)* in a screen for germline pattern defects. This recessive allele causes a highly penetrant, temperature-dependent Pro phenotype in which adult hermaphrodite germ lines contain a mass of cells proximal to gametes (Table 1, Fig. 2). Staining for mitosis-specific and germline-specific markers (see Materials and methods) confirmed that the proximal cells are mitotic germ cells (Fig. 3; data not shown). *pro-1(na48)* animals displayed additional non-Pro phenotypes (Table 1). The Pro phenotype was most penetrant at higher temperatures, and non-Pro defects increased in penetrance at lower temperatures and/or lower genetic dose. Overall, the genetic dosage and temperature analyses suggest that the *pro-1(na48)* Pro phenotype is a weak loss-of-function phenotype for this locus, and non-Pro phenotypes become more penetrant upon further reduction of *pro-1* activity. The *pro-1(na48)* Pro phenotype is a striking deviation from the normal spatial pattern of proliferation and differentiation in the germ line, therefore we focused our investigation on this phenotype.

The *pro-1(na48)* Pro phenotype results from a delay and displacement of initial meiosis

Different developmental mishaps can cause a Pro phenotype, including meiosis-to-mitosis reversal (Subramaniam and Seydoux, 2003) or defective initial meiosis (Pepper et al., 2003b). To determine the cellular basis for the Pro phenotype in *pro-1(na48)*, we conducted a time-course analysis of germline development (Table 2, Fig. 4). Initial meiosis was variable and delayed relative to somatic development: it occurred in the late L4/early adult as opposed to the L3 in wild type (Table 2). Unlike the wild type, where initial meiosis occurs in the proximal-most germ cells, it occurred at a further distal position in *pro-1(na48)*. Thus, at initial meiosis, meiotic entry separated the previously all-mitotic germ line into populations of (normal) distal mitotic and (ectopic) proximal mitotic germ cells. Meiotic development proceeded normally from distal cells into gametogenesis, and gametes accumulated distal to the tumor (Fig. 4).

To further test the possibility that some germ cells were entering meiosis and then reverting to mitosis, we examined *pro-1(na48); mpk-1(ga111)* double mutants. *mpk-1(ga111)* causes a pachytene exit defect (Pex) (Lackner and Kim, 1998). Therefore this mutation should suppress a Pro phenotype caused by reversion from meiosis to mitosis after pachytene. Both Pro and Pex phenotypes are expressed in *pro-1(na48);*

Table 1. Genetic dose and temperature dependence of *pro-1* mutant phenotypes

Genotype	Temperature (ºC)	Pro* (%)	Mig† (%)	Gametogenesis‡ (%)	Abnormal vulva§ (%)	*n*¶	Hours to adult molt**	Relative rate of development††
pro-1(+)	25	0	1	100	0	180	35.5	1
pro-1(+)/pro-1(na48)	25	0	1	100	0	112	35.5	1
pro-1(na48)	25	83	38	100	0	138	54	0.66
pro-1(na48)/Df‡‡	25	57	69	100	0	54	85	0.42
pro-1(RNAi)§§	25	1	53	73	Pvl 17	122	ND	ND
pro-1(+)	20	0	1	100	0	108	47.5	1
pro-1(+)/pro-1(na48)	20	0	1	100	0	126	47.5	1
pro-1(na48)¶¶	20	11	56	100	0	130	78	0.61
*pro-1(na48)/Df****	20	20	80	100	Vul 7, Pvl 21	56	~110	0.43
pro-1(+)	15	0	0	100	0	122	78	1
pro-1(+)/pro-1(na48)	15	0	0	100	0	118	78	1
pro-1(na48)	15	0	65	66	Pvl 9	114	~168	0.46
pro-1(na48)/Df	15	0	100	36	Vul 100	28	~240	0.33

*Mitotic germ cells proximal to gametes. In a separate experiment, 72 hours post-hatch-off, 63% of Pro arms (*n*=94; 72% Pro) contained both oocytes and sperm and remainder contained only sperm. At 96 hours, 84% of Pro arms (*n*=70; 71% Pro) contained both oocytes and sperm. Therefore, reduced oogenesis may reflect a delay in the spermatogenesis/oogenesis switch.

†Abnormal DTC migration. Defects seen in dorsal, centrifugal or both migrations. Mig and Pro did not correlate nor were they mutually exclusive.

‡Spermatocytes, sperm and/or oocyte nuclei observed with DAPI or Nomarski.

§Vul, Vulvaless; Pvl, protruding vulva (versus Evl, abnormally everted vulva).

¶*n*=number of gonad arms scored. For vulva phenotypes, the number of animals scored is *n*/2.

**Hours to adult molt from the hatch-off (see Materials and methods).

††Relative development rate: hours from hatch-off to adult molt in wild-type over mutant; ratio gives comparative rates of development at different temperatures.

‡‡*Df = mnDf58. pro-1(na48)/mnDf58* were synchronized non-GFP progeny of *pro-1(na48)/mIn1* males crossed to *mnDf58/mIn1* hermaphrodites. Pro data alone are inconsistent with *pro-1(na48)* as a simple reduction of function allele. This inconsistency may result from temperature-sensitive haploinsufficiency of another locus under the deficiency.

§§Data are reported from a single experiment (see Materials and methods); similar results were obtained from multiple RNAi experiments.

¶¶Although *pro-1(na48)* is only 11% Pro at 20ºC, the strain is difficult to maintain because of Emo sterility. Emo: 33%(29/86) of gonad arms, scored by DAPI at 120 hours post-hatch-off.

***One individual Vul *pro-1(na48)/mnDf58* animal displayed the Pro phenotype in both gonad arms.

ND, not determined.

mpk-1(ga111) double mutant animals (Table 3A), consistent with our time-course results and the conclusion that *pro-1(na48)* tumors derive from early pre-meiotic germ cells.

pro-1(na48) affects overall developmental rate: mutants reach the adult stage over 18 hours later than the wild type (Table 1). We asked how this defect related to germline development and found that the growth rate of the germ line was even more severely delayed in reference to somatic development benchmarks (Table 2). At somatic gonad primordium formation, germ cell numbers in *pro-1(na48)* were similar to wild type (12-13 germ cells/arm), but then diverged significantly. At initial meiosis (late L4/adult versus L3), distal stem cell numbers were comparable (63±14 versus 51±5) but *pro-1(na48)* contained more total germ cells because of the proximal tumor (89 versus 58). At the adult molt, *pro-1(na48)* contained approximately half the wild-type total number of

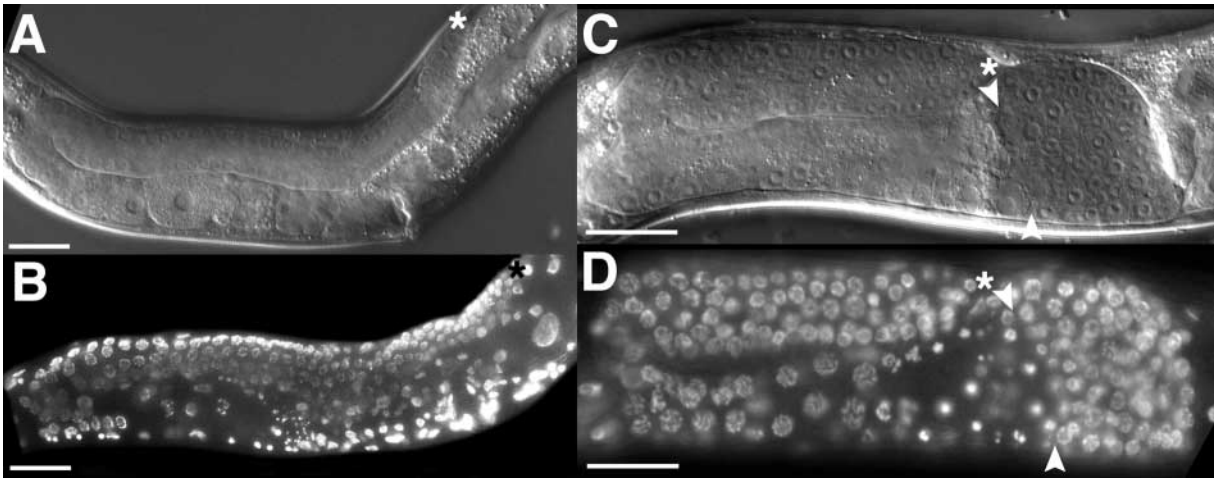

Fig. 2. The *pro-1(na48)* Pro phenotype. One gonad arm of adult hermaphrodites under Nomarski optics (A,C) and in fixed DAPI-stained whole worms (B,D). A,B and C,D are the same wild-type and *pro-1(na48)* individuals, respectively. Arrowheads indicate the abnormal gametogenesis/proximal mitosis border. Scale bars: 25 μm. Asterisks indicate the distal end of the gonad arms.

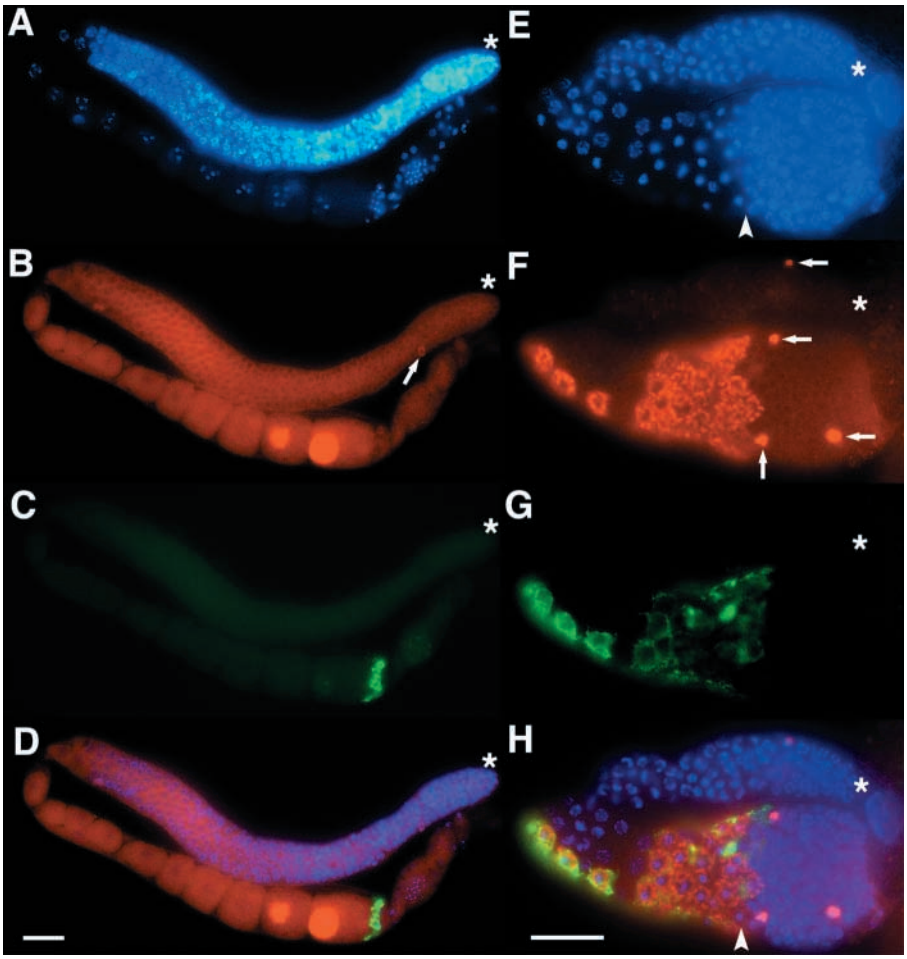

Fig. 3. Mitosis occurs within proximal undifferentiated germ cells in *pro-1(na48)* adults. Dissected gonad from adult wild-type (A-D) and *pro-1(na48)* (E-H) hermaphrodites labeled with DAPI (A,E), anti-phopho-histone H3 (B,F) and anti-MSP (C,G), and overlaid (D,H). Arrows (B,F) indicate M-phase mitotic nuclei (phospho-histone H3-positive/MSP-negative, non-oocyte). Arrowheads indicate the abnormal gametogenesis/proximal mitosis border. Scale bars: 25 μm. Asterisks indicate the distal end of the gonad arms.

germ cells, and these cells had not yet reached pachytene, whereas gametogenesis was already under way in wild type (Table 2). Gametogenesis did not occur in the majority of *pro-1(na48)* mutants until well into the adult stage (Fig. 4).

We examined the effect of sex determination on the Pro phenotype. *C. elegans* hermaphrodites first produce sperm and then switch to oogenesis, thus cells destined to become sperm are the first to enter meiosis. It is therefore possible that the proximal tumor in *pro-1(na48)* derives from male germ cells. We found that the *pro-1(na48)* Pro phenotype was still penetrant when the germ line was feminized by *fem-1(hc17)* (Nelson et al., 1978) (Table 3B), suggesting that the sexual identity of germ cells is irrelevant to tumor formation. *pro-1(na48)* males expressed the Pro phenotype at a significantly lower penetrance than hermaphrodites (Table 3C). This result suggests that differences between male and hermaphrodite gonadogenesis affect germline development.

The *pro-1(na48)* Pro phenotype depends on *glp-1* but not on the anchor cell

GLP-1 activity in the germ line promotes the mitotic fate and/or inhibits the meiotic fate (Austin and Kimble, 1987). In the absence of *glp-1*, all germ cells enter meiosis early. To determine if *glp-1* activity is required for the *pro-1(na48)* Pro phenotype, we assessed the phenotype of *pro-1(na48); glp-1(e2141ts)* double mutants. The double mutants displayed the *glp-1(loss-of-function)* phenotype, indicating that *glp-1* activity is required for the *pro-1(na48)* Pro phenotype (Table 3D). Because the GLP-1 receptor is activated by a somatic cell-produced ligand, this result is consistent with *pro-1(+)* acting upstream of or in parallel with *glp-1* in a regulatory pathway (therefore, possibly in the soma) or with a requirement for *glp-1* activity to generate enough germ cells for the *pro-1* Pro phenotype to manifest.

Some previously described Pro phenotypes are dependent on the anchor cell (AC) or its precursors, Z1.ppp and Z4.aaa. In these cases, this dependence is probably due to inappropriate proximal LAG-2/GLP-1 signaling (Seydoux et al., 1990; Pepper et al., 2003b). We used both genetic and physical cell ablations to ask if the *pro-1(na48)* Pro phenotype was dependent on the AC. No AC forms in *lin-12(n302)* mutants and this no-AC phenotype correlates directly with the vulvaless (Vul) phenotype (Greenwald et al., 1983). The Pro phenotype is penetrant in Vul animals (Table 3E), suggesting that an AC is not required for the *pro-1(na48)* tumor. LAG-2 produced by Z1.ppp and Z4.aaa signals to germ cells in the L2 (Pepper et al., 2003b). Therefore it remained possible that mitosis-promoting levels of LAG-2 were produced in the *pro-1(na48); lin-12(n302)* double mutant prior to the AC/VU decision. To eliminate this possibility, we ablated the precursors to these cells in *pro-1(na48)* (see Materials and methods). In 11 operated hermaphrodites 9/22 (41%), gonad arms displayed the Pro phenotype (in one animal both arms were Pro) compared with 26 unoperated control animals with 18/52 (35%) Pro. We conclude that LAG-2 produced by the AC or its precursors is not contributing to the *pro-1(na48)* Pro phenotype.

pro-1 encodes a WD-repeat-containing protein

To better understand the role of *pro-1*, we cloned the gene. We mapped *pro-1(na48)* to a physical interval containing 30 predicted ORFs (see Materials and methods). Genome-wide RNAi studies indicated that RNAi of R166.4 caused sterile, slow-growing and 'patchy coloration' phenotypes under low magnification (Kamath et al., 2003), consistent with our observations for *pro-1(na48)*. R166.4 genomic DNA from *pro-1(na48)* animals contained a single base change corresponding to a D211N substitution (see Materials and methods). D211 is highly conserved in phylogenetically diverse members of the

WD-repeat subfamily to which R166.4 belongs (Fig. 5) and is part of the consensus sequence for the WD-repeat motif (van der Voorn and Ploegh, 1992). Transgenic lines carrying R166.4-containing extrachromosomal arrays (see Materials and methods; 2/2 lines) rescued *pro-1(na48)* mutant phenotypes. We conclude from mapping, sequence and rescue data that R166.4 is *pro-1*. The transgenic rescue also suggested that *pro-1(+)* may function in the soma, given that simple arrays are silenced in the *C. elegans* germ line (Kelly et al., 1997).

The PRO-1 subfamily of WD-repeat containing proteins includes single apparent orthologs in representative protozoa, fungi, plants and animals (Fig. 5). The putative orthologs of PRO-1 are essential for viability in both fission yeast and

Table 2. Germ cell counts in *pro-1(na48)* and *pro-1(+)* per gonad arm at somatic- and germline-specific developmental time points

Developmental event	Genotype	Hours post hatch	Stage*	Distal mitosis	Transition	Pachytene	Gametes†	Proximal mitosis	Total germ nuclei	*n*
SPh‡	*pro-1(+)*	18	eL3	13±2	–	–	–	–	13	28
	pro-1(na48)	30	eL3	12±1	–	–	–	–	12	28
Initial meiosis	*pro-1(+)*	26	L3	51±5	7±3	–	–	–	58	16
	pro-1(na48)	48-54§	lL4	63±14	13±10	–	–	13±17	89	27
Adult molt	*pro-1(+)*	35.5	adult	130±8	28±8	59±9	22±5	–	239	10
	pro-1(na48)	54	adult	69±13	14±15	–	–	19±22	102	12

Average germ cell counts±1 s.d.
n, number of gonad arms scored.
*Stage: eL3, early L3; lL4, late L4.
†Sperm and spermatocytes are included. The number of gametes reported for this time point is equal to the number of spermatocytes plus one-quarter of the number of sperm. At the adult molt, *pro-1(+)* gonad arms contained an average of 16±3 spermatocytes and 22±22 sperm.
‡Formation of the hermaphrodite somatic gonad primordium.
§In *pro-1(na48)*, initial meiosis is variable with respect to somatic developmental stage. Therefore, animals from three time points were pooled (4/15, 16/33 and 7/12 germ lines contained meiotic nuclei at 48, 50 and 54 hours post-hatch off, respectively).

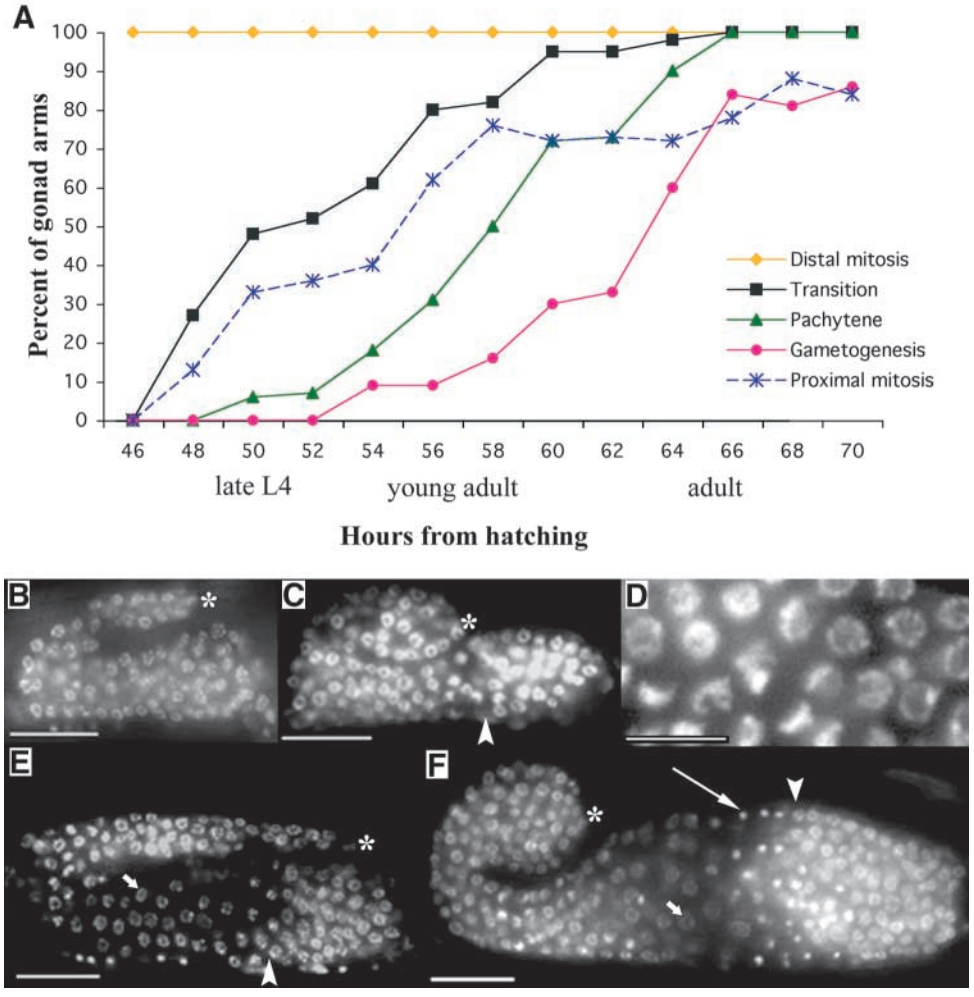

Fig. 4. Time-course analysis of the *pro-1(na48)* Pro phenotype. (A) Synchronized DAPI-stained animals (see Materials and methods) were scored for the presence of distal mitotic, transition, pachytene, gametogenic and proximal mitotic nuclei at indicated time points. Data are percent of gonad arms containing the indicated nuclei at a given time point. For each time point (46-70 hours at 2-hour intervals), *n*=62, 30, 66, 42, 58, 65, 38, 71, 60, 53, 80, 57 and 81 gonad arms, respectively. (B-F) One characteristic gonad arm from selected time points. (B) 52 hours: all-proliferative; (C) 58 hours: distal mitosis, transition and proximal mitosis; (D) higher-magnification view (different focal plane) of C to show transition nuclei (left) distal to mitotic nuclei (right); (E) 64 hours: distal mitotic, transition, pachytene and proximal mitotic nuclei; (F) 66 hours: gametogenesis just distal to proximal mitosis. Arrowheads indicate the abnormal gametogenesis/proximal mitosis border. Asterisks indicate the distal end of the gonad arms. Scale bars: 10 μm in D; 25 μm in B,C,E,F.

Table 3. *pro-1(na48)* genetic interactions and RNAi phenotypes

(A)	Genotype*,†	% Pro	% Pex	*n*
	pro-1(na48)	66	0	92
	mpk-1(ga111)	0	91	162
	pro-1(na48);mpk-1(ga111)	64‡	100	98
(B)	Genotype*,§,¶	% Pro	% Fem	*n*
	pro-1(na48)	58**	0	160
	fem-1(hc17)	0	100	152
	pro-1(na48); fem-1(hc17)	43	90††	171
(C)	Genotype*,§,‡‡	Hermaphrodite % Pro(*n*)	Male % Pro(*n*)	
	pro-1(na48); him-5(e1490)	74 (80)§§	23 (40)	
(D)	Genotype*,§,¶¶	% Pro	% Glp	*n*
	pro-1(na48)	84	0	62
	glp-1(e2141)	0	100	62
	pro-1(na48);glp-1(e2141)	0	100	88
(E)	Genotype*,§,***	% Pro	% Vul	*n*
	pro-1(na48)	75**	0	60
	lin-12(n302)	0	98	522
	pro-1(na48);lin-12(n302)	68	100	72
(F)	Genotype	% Gon†††	*n*	
	pro-1(RNAi)	100	122	
	rrf-1(pk1417); pro-1(RNAi)	6	296	
(G)	Genotype*,‡‡‡	% Pro at 20ºC	% Glp at 20ºC	*n*
	pro-1(na48)	11	0	82
	glp-1(e2141)	0	4	212
	pro-1(na48);glp-1(e2141)	0	31	58
(H)	Genotype*,§,§§§	% Pro at 20ºC	*n*	
	pro-1(na48)	19	208	
	glp-1(ar202)	0	152	
	pro-1(na48);glp-1(ar202)	72	118	

n, number of gonad arms; Vul, number of animals scored equals half *n*.

*Homozygous *pro-1(na48)*: self progeny of heterozygous parents balanced by *mIn1*.

†Strains marked with *unc-79(e1068)*, grown at 20ºC and shifted to 25ºC as gravid adults. L1 progeny were synchronized and cultured at 25ºC for 72 hours [*pro-1(na48)*-containing strains] or 48 hours, before fixation and DAPI staining. Pex (pachytene exit defect): mitotic, transition and pachytene nuclei present but no gametes.

‡Pro here is a Pro/Pex phenotype (see text).

§Strains marked with *unc-4(e120)*.

¶Strains grown at 20ºC. Synchronized L1 animals were shifted to 25ºC and scored after 72 hours (*pro-1(na48)*-containing strains) or 48 hours.

**These values are not significantly different ($P \geqslant 0.05$) from the corresponding values two rows directly below (two-sided Fisher exact test).

††Remaining 10% non-Fem animals were non-Pro, non-Fem.

‡‡Animals fixed and DAPI stained after 72 hours.

§§This value is significantly different from the value in the next column ($P<2\times10^{-7}$, based on two-sided Fisher exact test).

¶¶Strains marked with *dpy-17(e164)* and grown at 20ºC. Synchronized L1 animals were shifted to 25ºC.

***For *pro-1(na48)*-containing strains, mid-L4s were picked to a fresh plate and fixed and DAPI stained 24 hours later. For *unc-4(e120); lin-12(n302)*, all adults from several mixed-stage plates were scored under Normarki optics for Vul and Pro phenotypes.

†††Asynchronous adults scored for the Gon phenotype under Nomarski optics.

‡‡‡Strains homozygous for *him-5(e1490)*, grown at 20ºC, synchronized, fixed and DAPI stained after 72 hours for *glp-1(e2141); him-5(e1490)*, and after 96 hours for *pro-1(na48)*-containing strains.

§§§Animals grown at 20ºC, synchronized, fixed and DAPI-stained after 72 hours for *unc-4(e120); glp-1(ar202)*, and 96 hours for *pro-1(na48)*-containing strains.

budding yeast (Saka et al., 1997; Giaever et al., 2002), but the functional role of this protein in multicellular organisms is unexplored (see Discussion).

pro-1::GFP is widely expressed

To assess the *pro-1* expression pattern, we fused *pro-1* upstream sequences to GFP (Materials and methods). Three independent transgenic lines expressed GFP in the embryo and in every major post-embryonic lineage including the somatic gonad. Although we did not expect to observe germline expression with this transgene, microarray experiments indicate that R166.4 is expressed in the germ line (Reinke et al., 2000).

pro-1(RNAi) causes severe lineage defects in somatic gonad development

Our temperature and dose analyses indicated that *pro-1(na48)* is an hypomorphic allele with more severe and pleiotropic phenotypes at lower temperatures. To assess a stronger loss-of-function phenotype, we depleted PRO-1 by RNAi (see Materials and methods). The progeny of wild-type animals fed bacteria expressing dsRNA complementary to *pro-1* [hereafter referred to as *pro-1(RNAi)* animals] exhibited phenotypes we observed in *pro-1(na48)*, including Mig and Pro phenotypes (Table 1, Fig. 6). An additional striking phenotype was the absence of parts of the somatic gonad sheath, spermatheca and

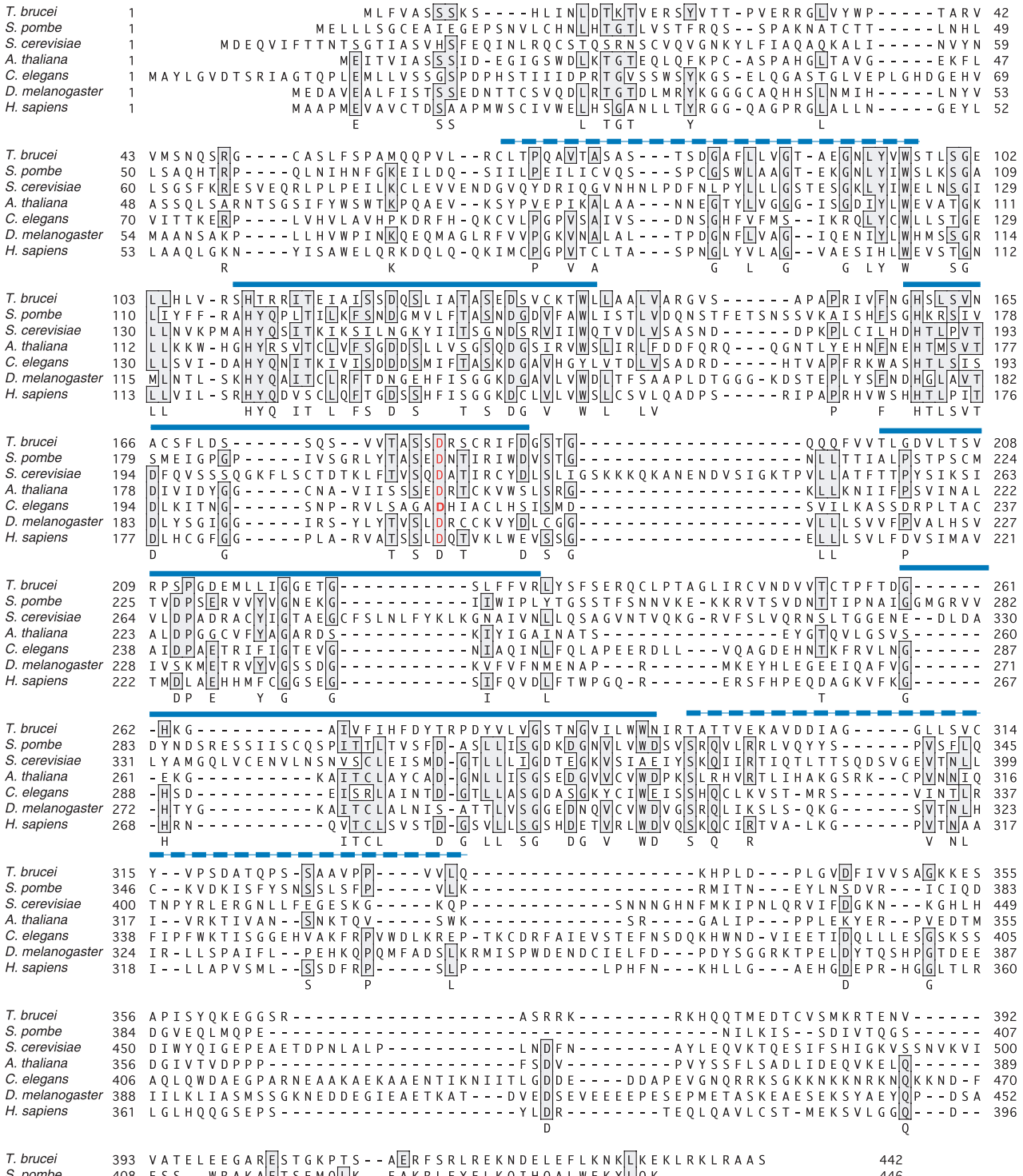

Fig. 5. PRO-1 is a member of a subfamily of WD-repeat proteins. Unbroken blue bars indicate WD-repeats in the underlying sequence (based on http://bmerc-www.bu.edu/wdrepeat/celegans/R166_CE_NEW.html); broken bars indicate possible degenerate repeats. The D211 residue is in red. Alignment from ClustalW (MacVector). Identical residues are boxed and shaded when present in more than four proteins; a consensus of these amino acids is given under the alignment. Sequences (NCBI locus names) are protozoan *T. brucei* (CAB95350), fission yeast *S. pombe* (NP_593710), budding yeast *S. cerevisiae* (NP_014217), plant *A. thaliana* (NP_190487), *C. elegans* (NP_496271), fly *D. melanogaster* (NP_569954) and *H. sapiens* (NP_077005). BLAST E-values against full-length PRO-1 range from 2.3×10^{-36} (human) to 1.9×10^{-10} (*S. cerevisiase*).

uterine lineages (Gon phenotype, Gonad development abnormal). Both DTCs and AC, however, were present (*n*=61 worms). The germ lines of *pro-1(RNAi)* animals were also severely under-proliferated, consistent with results of cell ablations that remove the spermatheca/sheath lineage (McCarter et al., 1997).

To further investigate the effects of *pro-1(RNAi)* on somatic gonad development, we analyzed the expression patterns of somatic gonad markers in *pro-1(RNAi)* worms. Out of 56 animals carrying *ajm-1::GFP*, a marker that exhibits a reproducible pattern in the spermatheca (Koppen et al., 2001), 20 did not express GFP in the spermatheca and 24 displayed obvious abnormalities in the spermathecal GFP expression pattern. Of 66 gonad arms of animals carrying *lim-7::GFP* (marking sheath cell pairs 1-4) (Hall et al., 1999), one arm expressed GFP in all eight cells, 42 arms in one or two cells, and in eight arms no sheath GFP was observed (Fig. 6). These results demonstrate that PRO-1 is required for the proper generation or differentiation of somatic gonad lineages.

To determine if the germline defects in *pro-1(RNAi)* animals were solely the result of depletion of PRO-1 in the soma, we examined *pro-1(RNAi)* animals in an *rrf-1(pk1417)* mutant background that strongly reduces RNAi in the soma, but permits RNAi in the germ line (Sijen et al., 2001). In contrast to our results in an *rrf-1(+)* background, *pro-1(RNAi)* treatment of *rrf-1(pk1417)* mutants produced fertile, non-Gon progeny (Table 3F). These results suggest that both germline and somatic defects in *pro-1(RNAi)* animals result from a depletion of PRO-1 in the soma.

The *pro-1(na48)* Pro phenotype is associated with a reduction of *pro-1* activity in the somatic gonad sheath/spermatheca lineage

Given our results suggesting that *pro-1* acts in the soma, we asked if anatomical somatic gonad defects would correlate with the Pro phenotype in *pro-1(na48)*. At 25°C, *pro-1(na48)* animals exhibited normal vulval, uterine and spermathecal morphology (*n*=69, 23 and 12, respectively; assayed by L4 vulva and uterus morphology under Nomarski optics and spermathecal *ajm-1::GFP* pattern). By contrast, sheath cell numbers were sometimes reduced, but this could not be directly correlated with the Pro phenotype. That is, some Pro animals displayed a reduction in the number of *lim-7::GFP*-positive or CEH-18-positive sheath cells (Greenstein et al., 1994), while others displayed the wild-type 8 *lim-7::GFP*-positive or 10 CEH-18-positive sheath cells (data not shown). Both gonadal sheath and gonad arms in *pro-1(na48)* Pro animals were often mis-shapen (Figs 2-4). We examined the sheath cell actin cytoskeleton by rhodamine-phalloidin staining (Strome, 1986; McCarter et al., 1997), and it appeared variably abnormal in both Pro and non-Pro animals (data not shown). We postulate that the *pro-1(na48)* Pro phenotype does not correlate with a sheath cell generation defect, but may correlate with defects in sheath cell growth, function and/or

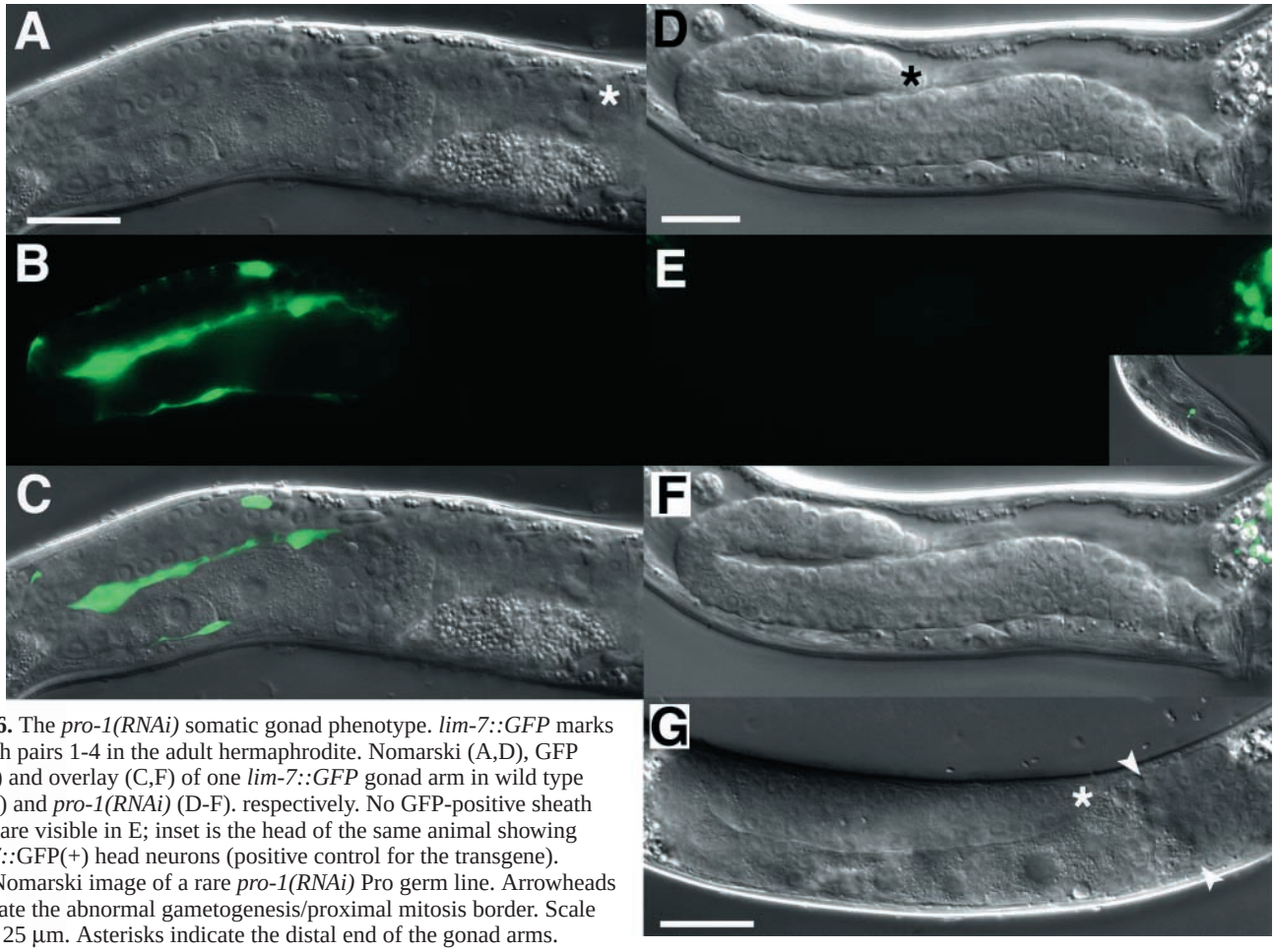

Fig. 6. The *pro-1(RNAi)* somatic gonad phenotype. *lim-7::GFP* marks sheath pairs 1-4 in the adult hermaphrodite. Nomarski (A,D), GFP (B,E) and overlay (C,F) of one *lim-7::GFP* gonad arm in wild type (A-C) and *pro-1(RNAi)* (D-F). respectively. No GFP-positive sheath cells are visible in E; inset is the head of the same animal showing *lim-7::*GFP(+) head neurons (positive control for the transgene). (G) Nomarski image of a rare *pro-1(RNAi)* Pro germ line. Arrowheads indicate the abnormal gametogenesis/proximal mitosis border. Scale bars: 25 μm. Asterisks indicate the distal end of the gonad arms.

aspects of differentiation dispensable for *lim-7* or *ceh-18* expression.

pro-1(+) is required in the sheath/spermatheca lineage to prevent the Pro phenotype

To determine the anatomical focus of *pro-1(+)* activity with respect to the Pro phenotype, we performed a genetic mosaic analysis (see Materials and methods); results are summarized in Fig. 7. Mosaic Pro animals and mosaic non-Pro animals were scored for lineages that had lost a transgenic array carrying *pro-1(+)* in *pro-1(na48)* animals. The array also contained *sur-5::GFP*, a cell-autonomous nuclear marker (Yochem et al., 1998). Independent mosaic Pro animals were identified that had lost the array in the entire P1, EMS or MS lineages, all of which contribute to the somatic gonad. Loss of the array in Z4 produced animals with a posterior Pro arm and an anterior non-Pro arm. Analysis of losses within the Z1 or Z4 lineages indicated that *pro-1(+)* must be present in the lineages descending from *both* of the SS cells within a given arm to prevent a Pro mutant phenotype in the neighboring germ line. Our data do not support a DTC role for *pro-1* vis-à-vis the Pro phenotype because we observed Pro gonad arms adjacent to a *pro-1(+)* DTC. For example, two mosaic Pro animals lost the array in Z1.p but retained it in Z1.a (similarly, for 4 Pro Z4.a/ Z4.p mosaics). The subsequent requirement for *pro-1(+)* in the sheath versus spermatheca lineage is difficult to distinguish by mosaic analysis (it would require one loss within each SS cell lineage in the same gonad arm), but because the SS cells and their daughters normally contact the L3 germ line during the time that germline pattern is established, it is likely that *pro-1(+)* is required in these cells.

Discussion

A defect in the somatic gonad sheath/spermatheca lineage disrupts germline pattern

We isolated *pro-1(na48)*, a reduction-of-function allele that causes proximal germline tumor formation. We found that this *pro-1(na48)* Pro phenotype stems from an earlier spatial and temporal defect in the developmental patterning of germline proliferation and differentiation. Three lines of evidence suggest that *pro-1(+)* acts in the somatic gonad, not the germ line. First, the Pro phenotype was rescued by a transgene that is likely silenced in the germ line (Kelly et al., 1997). Second, *pro-1(RNAi)* disrupted somatic gonad development in a somatic RNAi-dependent manner. Third, mosaic analysis in *pro-1(na48)* indicated that both SS cells in a gonad arm must possess *pro-1(+)* activity to ensure proper patterning of initial meiosis in the adjacent germ line.

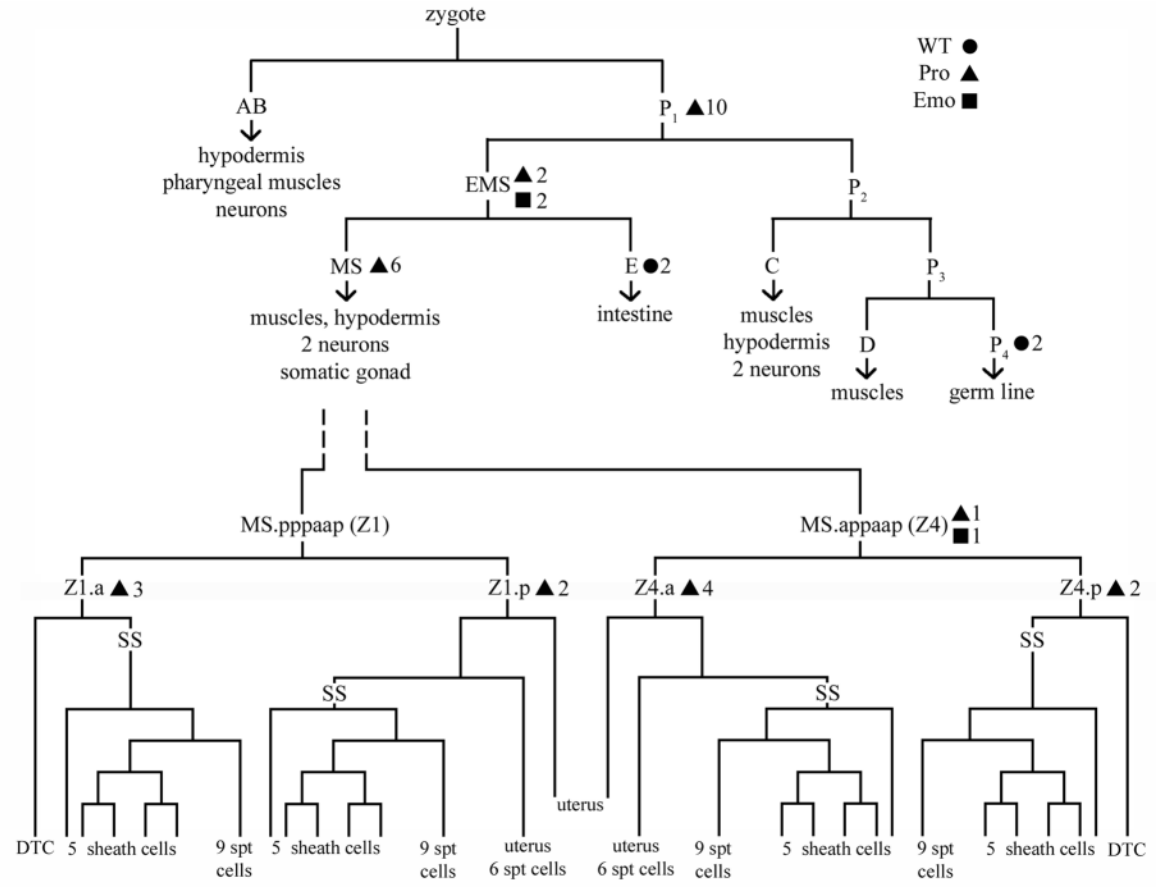

Fig. 7. *pro-1* mosaic analysis. Major embryonic lineages, somatic gonad lineages and the SS cells are shown. Broken lines indicate six divisions between MS and somatic gonad founders Z1 and Z4. Symbols are positioned at the youngest cell in which the transgenic array was lost, as indicated by GFP expression pattern (see text, and Materials and methods). Mosaic animals were scored wild type (circle), Pro (triangle) or Emo (square). For early losses, both gonad arms were scored. For losses within somatic gonad lineages, the phenotype of the gonad arm in which the array was lost is indicated.

The sheath/spermatheca lineage and the spatial and temporal control of proliferation and differentiation

The SS cells and their daughters are in a position to influence the neighboring germ line during the time that germline developmental pattern is established (Kimble and Hirsh, 1979; McCarter et al., 1997) (Fig. 1). Cell ablation of one or both SS cells per gonad arm (McCarter et al., 1997) is comparable with *pro-1* RNAi and mutant phenotypes. Ablation of both SS cells at the L2/L3 molt (prior to initial meiosis) causes defects in germline proliferation, pachytene exit and gametogenesis, similar to that observed in *pro-1(RNAi)* animals. Ablation of one of the two SS cells allows more robust proliferation but causes incompletely penetrant endomitotic oocytes (Emo) and feminization of the germ line (Fog) phenotypes (the Fog animals occasionally contain several proximal 'undifferentiated' germ cells that do not appear to proliferate and are likely defective in sexual fate specification) (McCarter et al., 1997). We never observed feminization of *pro-1(na48)* germ lines, but we did observe the Emo phenotype in non-Pro *pro-1(na48)* animals (Table 1), suggesting a defect in proximal sheath function (Greenstein et al., 1994; Rose et al., 1997; McCarter et al., 1999). Thus, SS lineage defects can confer complex phenotypes, some of which may preclude the identification of proliferation-dependent germline phenotypes. A clear understanding of the SS lineage/germline interaction vis-à-vis germline patterning may require further analysis of rare alleles.

Several models can accommodate results pertaining to an SS lineage function in overall proliferation and proliferation/differentiation patterning. One model is that the mitosis-promoting function (McCarter et al., 1997) is limited to the SS cells themselves, and the distal pair of SS cell progeny take on a mitosis-inhibiting/meiosis-promoting function after they are born (Fig. 1, Fig. 8A). Another possibility is that the proximal SS cell daughters take on a mitosis-inhibiting/meiosis-promoting function while the distal progeny promote mitosis (Fig. 8B). Together with a critical distance from the DTC, either mechanism could ensure that the mitosis/meiosis border is sharp and that meiotic entry is reproducibly positioned in the proximal-most germ line, adjacent to the somatic gonad.

In these scenarios, the *pro-1(na48)* mutation could augment or prolong a mitosis-promoting function of the SS cells (or either daughters), or it could disable or delay a mitosis-inhibiting function of either SS daughter. The first possibility would lead to a cell-dominant effect that is consistent with our finding that mosaic gonad arms with a sheath and spermatheca composed of cells that were half *pro-1(na48)* and half *pro-1(+)* displayed the Pro phenotype. Previous observations suggest that once proximal germline proliferation occurs later than the normal time of initial meiosis, the proximal germline environment is permissive for continued mitosis (Seydoux et al., 1990; Francis et al., 1995; Qiao et al., 1995; Subramaniam and Seydoux, 2003; Pepper et al., 2003a; Pepper et al., 2003b). Thus, we propose that any normal mitosis-promoting function of the early SS lineage cells must be temporally and spatially restricted.

In its *pro-1*-dependent role in preventing proximal proliferation, the SS lineage could indirectly facilitate or maintain the downregulation of GLP-1-mediated signaling. Although our data do not rule out this mechanism, *pro-1(na48)* enhanced both *glp-1(loss-of-function)* Glp and *glp-1(gain-of-function)* Pro phenotypes (Table 3G,H), a result that is inconsistent with this simple interpretation. Alternatively, the later SS cell progeny could indirectly upregulate meiosis-promoting functions in the germ line (such as *gld-1* and *gld-2* pathways) (Kadyk and Kimble, 1998).

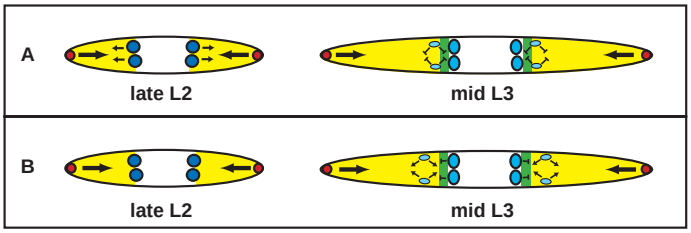

Fig. 8. Models for proposed SS lineage involvement in regulation of initial meiosis. All germ cells are mitotic in the L2 and meiotic onset occurs in the L3. See text for discussion of models depicted in A and B.

An alternate but not mutually exclusive model is that the SS lineage provides a structural, physiological or nutritional role that is necessary for normal germline patterning, and that the *pro-1(na48)* mutation interferes with this role. EM studies on the distal sheath reveal prominent Golgi apparatus, endoplasmic reticulum and vesicles, suggestive of a secretory function for these cells (Hall et al., 1999). Regardless of the exact mechanism by which PRO-1 acts, our results provide a molecular in-road into a previously uncharacterized SS lineage-to-germline interaction that influences the pattern of germline proliferation and differentiation without perturbing germ cell fate acquisition.

PRO-1 and putative orthologs likely play roles in many cellular processes

PRO-1 belongs to a subfamily of WD-repeat-containing proteins and has one putative ortholog in representatives of every major eukaryotic phylogenetic group. Apparent yeast orthologs of PRO-1 are Crb3 in *Schizosaccharomyces pombe* and IPI3 in *Saccharomyces cerevisiae*. These proteins are essential for viability (Saka et al., 1997; Giaever et al., 2002), and a conditional allele of IPI3 suggests a role in ribosome biogenesis (Peng et al., 2003). IPI3-interacting proteins have been identified (Ito et al., 2001; Gavin et al., 2002; Ho et al., 2002), and include 12 proteins involved in a variety of functions such as ribosome biogenesis, cell-cycle, kinase regulation, nucleocytoplasmic transport, chromatin assembly and ubiquitination. Because this information does not pinpoint a clear molecular role for *C. elegans* PRO-1, it will be of considerable interest to identify proteins that functionally and physically interact with PRO-1.

We gratefully acknowledge the technical assistance of John Maciejowski, the CGC for strains, gifts of reagents and/or strains from D. Greenstein, B. Grant, S. Strome, and Y. Kohara. Thanks also to T. Schedl, A. Pepper, S. Small, C. Desplan, R. Lehmann, and members of the Fitch and Piano laboratories for discussions. This work was supported by the NIH (GM61706 to E.J.A.H. and Developmental Genetics Program training grant T32HD07520).

References

Austin, J. and Kimble, J. (1987). *glp-1* is required in the germ line for regulation of the decision between mitosis and meiosis in C. elegans. *Cell* **51**, 589-599.

Brenner, S. (1974). The genetics of *Caenorhabditis elegans*. *Genetics* **77**, 71-94.

Brinster, R. L. (2002). Germline stem cell transplantation and transgenesis. *Science* **296**, 2174-2176.

Edgley, M. L. and Riddle, D. L. (2001). LG II balancer chromosomes in *Caenorhabditis elegans*: *mT1*(II;III) and the mIn1 set of dominantly and recessively marked inversions. *Mol. Genet. Genomics* **266**, 385-395.

Francis, R., Barton, M., Kimble, J. and Schedl, T. (1995). *gld-1*, a tumor suppressor gene required for oocyte development in *Caenorhabditis elegans. Genetics* **139**, 579-606.

Gavin, A. C., Bosche, M., Krause, R., Grandi, P., Marzioch, M., Bauer, A., Schultz, J., Rick, J. M., Michon, A. M., Cruciat, C. M. et al. (2002). Functional organization of the yeast proteome by systematic analysis of protein complexes. *Nature* **415**, 141-147.

Giaever, G., Chu, A. M., Ni, L., Connelly, C., Riles, L., Veronneau, S., Dow, S., Lucau-Danila, A., Anderson, K., Andre, B. et al. (2002). Functional profiling of the *Saccharomyces cerevisiae* genome. *Nature* **418**, 387-391.

Greenstein, D., Hird, S., Plasterk, R. H., Andachi, Y., Kohara, Y., Wang, B., Finney, M. and Ruvkun, G. (1994). Targeted mutations in the Caenorhabditis elegans POU homeo box gene *ceh-18* cause defects in oocyte cell cycle arrest, gonad migration, and epidermal differentiation. *Genes Dev.* **8**, 1935-1948.

Greenwald, I., Sternberg, P. and Horvitz, H. (1983). The *lin-12* locus specifies cell fates in Caenorhabditis elegans. *Cell* **34**, 435-444.

Hall, D. H., Winfrey, V. P., Blaeuer, G., Hoffman, L. H., Furuta, T., Rose, K., Hobert, O. and Greenstein, D. (1999). Ultrastructural features of the adult hermaphrodite gonad of *Caenorhabditis elegans*: relations between the germ line and soma. *Dev. Biol.* **212**, 101-123.

Henderson, S., Gao, D., Lambie, E. and Kimble, J. (1994). *lag-2* may encode a signaling ligand for the GLP-1 and LIN-12 receptors of *C. elegans*. *Development* **120**, 2913-2924.

Ho, Y., Gruhler, A., Heilbut, A., Bader, G. D., Moore, L., Adams, S. L., Millar, A., Taylor, P., Bennett, K., Boutilier, K. et al. (2002). Systematic identification of protein complexes in *Saccharomyces cerevisiae* by mass spectrometry. *Nature* **415**, 180-183.

Ito, T., Chiba, T., Ozawa, R., Yoshida, M., Hattori, M. and Sakaki, Y. (2001). A comprehensive two-hybrid analysis to explore the yeast protein interactome. *Proc. Natl. Acad. Sci. USA* **98**, 4569-4574.

Kadyk, L. and Kimble, J. (1998). Genetic regulation of entry into meiosis in *Caenorhabditis elegans*. *Development* **125**, 1803-1813.

Kamath, R. S., Fraser, A. G., Dong, Y., Poulin, G., Durbin, R., Gotta, M., Kanapin, A., le Bot, N., Moreno, S., Sohrmann, M. et al. (2003) Systematic functional analysis of the *Caenorhabditis elegans* genome using RNAi. *Nature* **421**, 231-237.

Kawasaki, I., Shim, Y. H., Kirchner, J., Kaminker, J., Wood, W. B. and Strome, S. (1998). PGL-1, a predicted RNA-binding component of germ granules, is essential for fertility in C. elegans. *Cell* **94**, 635-645.

Kelly, W., Xu, S., Montgomery, M. and Fire, A. (1997). Distinct requirements for somatic and germline expression of a generally expressed *Caenorhabditis elegans* gene. *Genetics* **146**, 227-238.

Kiger, A. A. and Fuller, M. (2001). Male germ-line stem cells. In *Stem Cell Biology* (ed. D. R. Marshak, R. L. Gardner and D. Gottlieb), pp.149-187. Cold Spring Harbor, New York: Cold Spring Harbor Laboratory Press.

Kimble, J. and Hirsh, D. (1979). The postembryonic cell lineages of the hermaphrodite and male gonads in *Caenorhabditis elegans*. *Dev. Biol.* **70**, 396-417.

Kimble, J. and White, J. (1981). On the control of germ cell development in *Caenorhabditis elegans*. *Dev. Biol.* **81**, 208-219.

Kodoyianni, V., Maine, E. and Kimble, J. (1992). Molecular basis of loss-of-function mutations in the *glp-1* gene of *Caenorhabditis elegans*. *Mol. Biol. Cell* **3**, 1199-1213.

Koppen, M., Simske, J. S., Sims, P. A., Firestein, B. L., Hall, D. H., Radice, A. D., Rongo, C. and Hardin, J. D. (2001). Cooperative regulation of AJM-1 controls junctional integrity in *Caenorhabditis elegans* epithelia. *Nat. Cell Biol.* **3**, 983-991.

Lackner, M. R. and Kim, S. K. (1998). Genetic analysis of the *Caenorhabditis elegans* MAP kinase gene *mpk-1*. *Genetics* **150**, 103-117.

Lambie, E. J. and Kimble, J. (1991). Two homologous regulatory genes, *lin-12* and *glp-1*, have overlapping functions. *Development* **112**, 231-40.

McCarter, J., Bartlett, B., Dang, T. and Schedl, T. (1997). Soma-germ cell interactions in *Caenorhabditis elegans*: multiple events of hermaphrodite germline development require the somatic sheath and spermathecal lineages. *Dev. Biol.* **181**, 121-143.

McCarter, J., Bartlett, B., Dang, T. and Schedl, T. (1999). On the control of oocyte meiotic maturation and ovulation in *Caenorhabditis elegans*. *Dev. Biol.* **205**, 111-128.

McLaren, A. (2003). Primordial germ cells in the mouse. *Dev. Biol.* **262**, 1-15.

Mello, C. and Fire, A. (1995). DNA transformation. *Methods Cell Biol.* **48**, 451-482.

Miller, M. A., Nguyen, V. Q., Lee, M. H., Kosinski, M., Schedl, T., Caprioli, R. M. and Greenstein, D. (2001). A sperm cytoskeletal protein that signals oocyte meiotic maturation and ovulation. *Science* **291**, 2144-2147.

Morgan, P. G., Sedensky, M., Meneely, P. M. (1990). Multiple sites of action of volatile anesthetics in *Caenorhabditis elegans*. *Proc. Natl. Acad. Sci. USA* **87**, 2965-2969.

Nelson, G. A., Lew, K. K. and Ward, S. (1978). Intersex, a temperature-sensitive mutant of the nematode *Caenorhabditis elegans*. *Dev. Biol.* **66**, 386-409.

Peng, W. T., Robinson, M. D., Mnaimneh, S., Krogan, N. J., Cagney, G., Morris, Q., Davierwala, A. P., Grigull, J., Yang, X., Zhang, W. et al. (2003). A panoramic view of yeast noncoding RNA processing. *Cell* **113**, 919-933.

Pepper, A. S., Killian, D. J. and Hubbard, E. J. (2003a). Genetic analysis of *Caenorhabditis elegans glp-1* mutants suggests receptor interaction or competition. *Genetics* **163**, 115-132.

Pepper, A. S., Lo, T. W., Killian, D. J., Hall, D. H. and Hubbard, E. J. (2003b). The establishment of *Caenorhabditis elegans* germline pattern is controlled by overlapping proximal and distal somatic gonad signals. *Dev. Biol.* **259**, 336-350.

Qiao, L., Lissemore, J., Shu, P., Smardon, A., Gelber, M. and Maine, E. (1995). Enhancers of *glp-1*, a gene required for cell-signaling in *Caenorhabditis elegans*, define a set of genes required for germline development. *Genetics* **141**, 551-569.

Reinke, V., Smith, H. E., Nance, J., Wang, J., van Doren, C., Begley, R., Jones, S. J., Davis, E. B., Scherer, S., Ward, S. et al. (2000). A global profile of germline gene expression in *C. elegans*. *Mol. Cell* **6**, 605-616.

Rose, K. L., Winfrey, V. P., Hoffman, L. H., Hall, D. H., Furuta, T. and Greenstein, D. (1997). The POU gene ceh-18 promotes gonadal sheath cell differentiation and function required for meiotic maturation and ovulation in *Caenorhabditis elegans*. *Dev. Biol.* **192**, 59-77.

Saka, Y., Esashi, F., Matsusaka, T., Mochida, S. and Yanagida, M. (1997). Damage and replication checkpoint control in fission yeast is ensured by interactions of Crb2, a protein with BRCT motif, with Cut5 and Chk1. *Genes Dev.* **11**, 3387-3400.

Seydoux, G., Schedl, T. and Greenwald, I. (1990). Cell-cell interactions prevent a potential inductive interaction between soma and germline in C. elegans. *Cell* **61**, 939-951.

Sigurdson, D., Spanier, G. and Herman, R. (1984). *Caenorhabditis elegans* deficiency mapping. *Genetics* **108**, 331-345.

Sijen, T., Fleenor, J., Simmer, F., Thijssen, K. L., Parrish, S., Timmons, L., Plasterk, R. H. and Fire, A. (2001). On the role of RNA amplification in dsRNA-triggered gene silencing. *Cell* **107**, 465-476.

Spradling, A., Drummond-Barbosa, D. and Kai, T. (2001). Stem cells find their niche. *Nature* **414**, 98-104.

Strome, S. (1986). Fluorescence visualization of the distribution of microfilaments in gonads and early embryos of the nematode Caenorhabditis elegans. *J. Cell Biol.* **103**, 2241-2252.

Subramaniam, K. and Seydoux, G. (2003). Dedifferentiation of Primary Spermatocytes into Germ Cell Tumors in C. elegans Lacking the Pumilio-like Protein PUF-8. *Curr. Biol.* **13**, 134-139.

Tax, F., Yeargers, J. and Thomas, J. (1994). Sequence of *C. elegans* lag-2 reveals a cell-signalling domain shared with Delta and Serrate of Drosophila. *Nature* **368**, 150-154.

Timmons, L. and Fire, A. (1998). Specific interference by ingested dsRNA. *Nature* **395**, 854.

Timmons, L., Court, D. L. and Fire, A. (2001). Ingestion of bacterially expressed dsRNAs can produce specific and potent genetic interference in Caenorhabditis elegans. *Gene* **263**, 103-112.

van der Voorn, L., and Ploegh, H. L. (1992). The WD-40 repeat. *FEBS Lett.* **307**, 131-134.

Wicks, S. R., Yeh, R. T., Gish, W. R., Waterston, R. H. and Plasterk, R. H. (2001). Rapid gene mapping in Caenorhabditis elegans using a high density polymorphism map. *Nat. Genet.* **28**, 160-164.

Yochem, J., Gu, T. and Han, M. (1998). A new marker for mosaic analysis in *Caenorhabditis elegans* indicates a fusion between hyp6 and hyp7, two major components of the hypodermis. *Genetics* **149**, 1323-1334.